

See discussions, stats, and author profiles for this publication at: <https://www.researchgate.net/publication/232084794>

Hemiphasmidic Side-Chain Liquid Crystalline Polymer: From Smectic C Phase to Columnar Phase with a Bundle of Chains as Its Building Block

ARTICLE in ACS MACRO LETTERS · MAY 2012

Impact Factor: 5.76 · DOI: 10.1021/mz3001435

CITATIONS

13

READS

45

6 AUTHORS, INCLUDING:



Xiaofang Chen

Soochow University (PRC)

151 PUBLICATIONS 2,042 CITATIONS

[SEE PROFILE](#)



S. Yang

Peking University

39 PUBLICATIONS 329 CITATIONS

[SEE PROFILE](#)

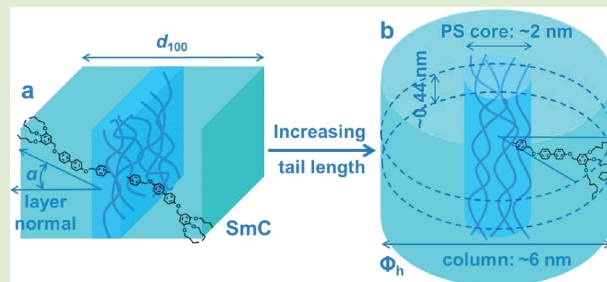
Hemiphasmidic Side-Chain Liquid Crystalline Polymer: From Smectic C Phase to Columnar Phase with a Bundle of Chains as Its Building Block

Jun-Feng Zheng, Xin Liu, Xiao-Fang Chen, Xiang-Kui Ren, Shuang Yang,* and Er-Qiang Chen*

Beijing National Laboratory for Molecular Sciences, Department of Polymer Science and Engineering and Key Laboratory of Polymer Chemistry and Physics of Ministry of Education, College of Chemistry, Peking University, Beijing 100871, China

Supporting Information

ABSTRACT: We synthesized a new hemiphasmidic side-chain liquid crystalline polymer ($P-n$, n is the number of carbons in alky tail of the side chain, $n = 4–12$) using free radical polymerization. The side chain of $P-n$ has a biphenyl in the middle, linked to the polystyrene backbone and to the terminal phenyl group with three alkyl tails via only methyleneoxy units. Upon increasing n , the mesophase of $P-n$ changes from bilayer smectic C to hexagonal columnar (Φ_h) phase with the a -dimension of ~ 6 nm. Both of the mesophases are long-range ordered, which can be well aligned by simple shearing. The oriented Φ_h shows a quite low rotational disorder around the shear direction. Most likely, the Φ_h phase takes a bundle of chains (e.g., \sim five chains) rather than a single chain as its building block. This “multi-chain model” of the Φ_h phase may represent a new type of self-assembly in side-chain polymers.



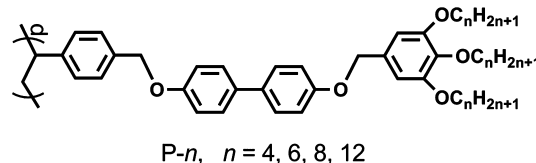
The design of functional materials based on molecular self-assembly attracts a great amount of interest because of its important applications in nanotechnologies.¹ Microphase separation of block copolymers can render a variety of ordered structures,² which is considered as a promising “bottom-up” method for the nanofabrication process.³ The directed self-assembly of a block copolymer enables the formation of long-range ordered patterns with a periodicity of ~ 20 nm; further reducing the size down to ~ 10 nm can be achieved by further lowering the molecular weight (MW) of the block copolymer.³ Microphase separation also exists in side-chain polymers (SCPs), which can lead to a one-dimensionally (1D) ordered smectic phase⁴ or a two-dimensionally (2D) ordered columnar (Φ) phase.⁵ Considering a smectic phase of a SCP containing rodlike mesogens, the parallel packing of mesogens may dominate the layer structure, wherein the incompatible backbones form a sublayer squeezed by two adjacent side-chain sublayers.^{4c} For the Φ phase of SCPs, each column usually consists of a single chain with a cylinderlike conformation as a whole. The microphase separation along the radial direction can give the molecular cylinder a core–shell structure.^{5b–e} Regarding the construction of hierarchical structures 5–10 nm in size, SCPs may also be employed as templates or as nanostructured functional materials.

The periodicity and symmetry of SCP mesophases are largely determined by the side-chain structure. With rodlike mesogens such as biphenyl, the smectic layer spacing is of a few nanometers; increasing the mesogen length will certainly give a larger spacing.⁴ The Φ phase of SCP is often observed in dendronized polymers^{5b,c,e} and mesogen-jacketed liquid

crystalline (LC) polymers.^{5d,7} The diameter of the molecular cylinder can be adjusted by varying the side-chain structure. For example, a higher generation of dendritic side chain results in a thicker molecular cylinder of dendronized polymer.⁸ A single chain of the fifth-generation dendronized polymer can even possess a diameter close to ~ 10 nm.^{8d} Hemiphasmidic SCPs were first reported by Ringsdorf⁹ and by Percec,¹⁰ which can also form smectic and Φ phases. As the phasmid or polycatenar mesogen composed of a rodlike mesogen and a “half-disc” end group is larger than the conventional one, they provide larger periodicity to the resulted LC phases with different symmetries.^{9–11}

Here we design and synthesize a new hemiphasmidic side chain LC polymer (see Chart 1, denoted as $P-n$, where n is the

Chart 1. Chemical Structure of $P-n$



number of carbons in the alky tail), which is a derivative of polystyrene (PS) and can be obtained by simple chemistry. To

Received: March 23, 2012

Accepted: April 17, 2012

Published: April 26, 2012

improve the self-assembly ability, two methyleneoxy linkages are introduced to the side chain, leading to a flexible mesogenic structure.¹² However, no other flexible spacer is used between the PS backbone and the biphenyl group. P-*n* can form well-ordered LC phases. While P-4 and P-6 adopt a bilayer smectic C (SmC) structure, P-8 and P-12 show a long-range ordered hexagonal Φ (Φ_h) phase with the *a*-dimension of ~ 6 nm. We consider that the column of Φ_h phase is formed by a bundle of chains. Owing to its nature of SCP, P-*n* can be well aligned by simple mechanical shearing.

Detailed synthesis and characterization of the monomers and polymers are described in the Supporting Information (SI). Number average MWs of P-*n* were measured by gel permeation chromatography (GPC) using PS standards, which are $\sim 1.0 \times 10^5$ g/mol with the polydispersity of ~ 2 (see the SI). The phase behaviors of P-*n* were studied by differential scanning calorimetry (DSC), polarized optical microscopy (POM), and X-ray diffraction (XRD). Reconstruction of relative electron density maps was performed based on XRD results. The sample densities were measured by a flotation technique.

Figure 1a shows the DSC traces of P-*n* obtained by the second heating scan at $10^\circ\text{C}/\text{min}$. The glass transition

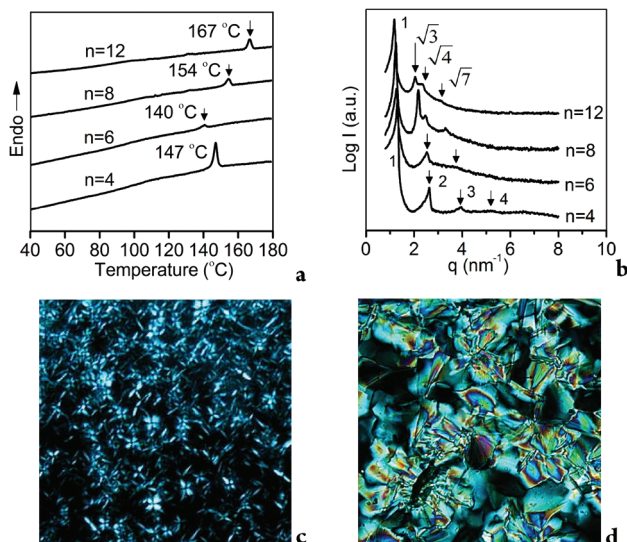


Figure 1. DSC traces of second heating scan (a) and 1D XRD patterns recorded at room temperature (b) of P-*n*. (c and d) POM images of LC textures of P-4 and P-8, respectively.

temperatures of P-*n* decrease with increasing *n*. All the samples show a single first-order transition, which is enantiotropic one that can be detected upon both cooling and heating (see the SI). The transition temperature decreases first and then increases with increasing *n*, implying that the samples with enough high MW may have distinct LC phases. LC textures of P-*n* were observed under POM after the samples were slowly cooled to temperatures slightly below the transition temperatures followed by prolonged annealing. As shown in Figure 1c,d, P-4 and P-8 exhibit different textures with the characteristics of smectic and Φ phase, respectively.

To identify the phase structures of P-*n*, both 1D and 2D XRD experiments were carried out. As shown in Figure 1b, the 1D XRD pattern of P-4 renders the diffractions with a *q*-ratio of 1:2:3:4 ($q = 4\pi \sin \theta/\lambda$, where λ is the X-ray wavelength and 2θ the scattering angle), a manifestation of the smectic phase. P-6 also displays the smectic diffractions. In the cases of P-8 and P-12,

the *q*-ratio of diffractions follows 1:3^{1/2}:4^{1/2}:7^{1/2}, featuring a Φ_h phase. All the samples had a scattering halo in the high-angle region with the maximum position corresponding to ~ 0.44 nm, indicating only short-range order existed at the subnanometer scale. The values of smectic layer spacing (*d*) and *a*-dimension of Φ_h phase of P-*n* based on the XRD measurements are summarized in Table 1.

Table 1. XRD Results, Estimated Side-Chain Lengths (*l_{sc}*, Here the Phenyl Group of the PS Backbone is Included), and Experimental Densities (ρ_{exp}) of P-*n*s

	P-4 (SmC)	P-6 (SmC)	P-8 (Φ_h)	P-12 (Φ_h)
<i>d</i> (SmC, nm)	4.79	4.94		
<i>a</i> (Φ_h , nm)			5.90	6.30
<i>l_{sc}</i> (nm)	2.74	2.97	3.21	3.70
ρ_{exp} (g/cm ³)	1.07	1.05	1.02	0.95

The diffractions up to the fourth order illustrate that P-*n* without traditional flexible spacer can exhibit perfect LC ordering. Compared with hemiphasmidic SCPs reported before,^{9,10} P-*n* possesses a flexible rodlike mesogen rather than a fully rigid one. The methyleneoxy units at both ends of the biphenyl provide additionally internal degree of freedom, allowing the side chains to adopt comfortable conformation and orientation to accomplish the self-assembly. Within the well-ordered LC phases of P-*n*, different components of the molecule should be segregated. Increasing *n* can alter the size and also the shape of the side chain, resulting in the phase changing from smectic to Φ_h , similar to that reported by Percec.^{10b} Here we intend to discuss in detail the phase structure of P-*n*.

Figure 2a depicts a 2D XRD pattern of P-4 at room temperature. The sample was oriented by shearing at 150°C

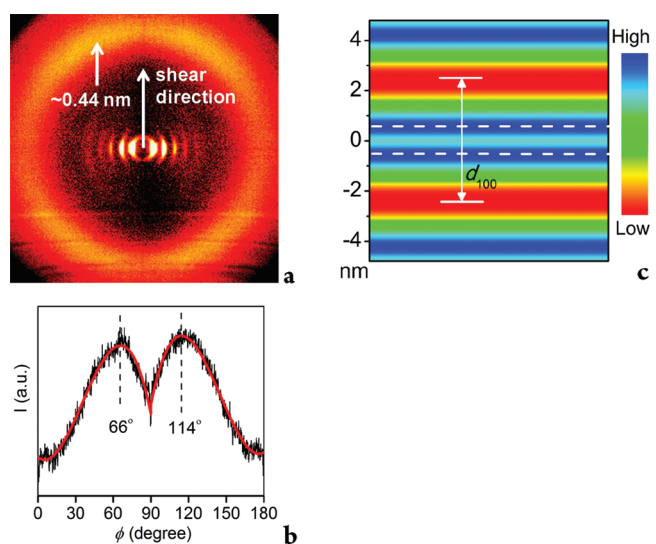


Figure 2. (a) 2D XRD pattern of an oriented P-4 sample. The shear direction is along the meridian. (b) The azimuthal scanning data (ϕ is the azimuthal angle) of the high-angle scattering shown in the upper part of (a). ϕ of 0° and 90° correspond to the equator and the meridian, respectively. (c) Relative electron density map of SmC structure of P-4. The white dashed line indicates the location of the highest electron density.

followed by annealing at 110°C . With the shear direction on the meridian, the layer diffractions up to the fifth order appear

on the equator. In the high-angle region, four arcs of ~ 0.44 nm are in the quadrants, which shall mainly come from the interference between side chains parallel to each other. The azimuthal scanning data of these arcs revealed that the side-chain axis was $\sim 25^\circ$ tilted with respect to the smectic layer normal (Figure 2b). Therefore, the 2D XRD result indicates a SmC structure. With an assumption that the side chain (here including the phenyl of PS backbone) adopts an extended conformation, the side-chain length (l_{SC} , see Table 1) of P-4 is estimated to be 2.74 nm. As the d_{100} of P-4 is rather close to $2l_{SC} \times \cos 25^\circ$, the SmC is a bilayer one (see the schematic in Figure 4a).

The reconstructed relative electron density map of P-4 is shown in Figure 2c. It is reasonable to assign the zone with low electron density (red colored) to the alkyl tails, the zone with high electron density (blue colored) to the rodlike mesogens, and the region squeezed between two adjacent blue zones to the backbones. For P-6, our 2D XRD result and reconstructed relative electron density map (see the SI) gave the results similar to that of P-4. However, the side chain of P-6 tilts $\sim 30^\circ$. Namely, for the SmC of P- n , larger n causes more tilt of the side chain. The longer alkyl tail usually adopts a more coiled conformation, resulting in the more wedge-shaped hemiphasmidic side-chain which demands larger interfacial area. For the layer structure with a nearly flat interface, increasing the chain tilt angle is a way to meet this requirement.¹³

However, further increasing the tail length leads to the Φ_h phase, as evidenced by the 1D XRD results of P- n with $n \geq 8$. 2D XRD experiments of oriented P-8 elucidate more clearly the hexagonal packing (Figure 3). The sample was prepared by

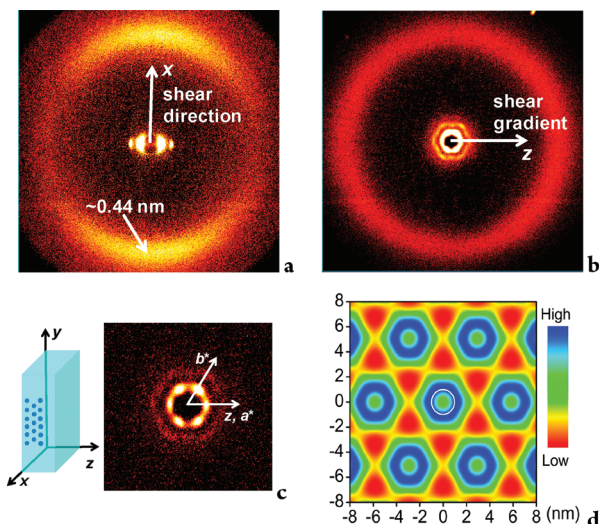


Figure 3. 2D XRD patterns of an oriented P-8 sample with X-ray beam perpendicular (a) and parallel (b) to the shear direction (x -direction), respectively. (c) Schematic of the sheared sample and 2D XRD pattern with an X-ray beam parallel to x recorded using short exposure time. The blue dot represents the column within the sample; the axes of x and z are the shear direction and shear gradient, respectively. (d) Relative electron density map of 2D hexagonal lattice of P-8. The white circle indicates the size of PS core.

shearing at 160 °C on a solid substrate followed by annealing at 110 °C. The film sample orientation is schematically drawn in Figure 3c, with the x - and z -direction representing the shear direction and the shear gradient, respectively. Figure 3a depicts

a 2D XRD pattern recorded with the X-ray beam perpendicular to x . While x is along the meridian, the $(hk0)$ diffractions of the Φ_h phase are located on the equator, and the high-angle scattering of ~ 0.44 nm is more or less concentrated on the meridian. This indicates that the columns are well parallel to x , and the side chains are largely perpendicular to the column axis.

In particular, when setting the sample vertically and letting X-ray beam go through x (see Figure 3c), we observe 6-fold symmetry of the $(hk0)$ diffractions as shown in Figure 3b. Figure 3c also depicts the low-angle diffractions recorded with shorter exposure time, demonstrating more clearly that the a^* of hexagonal lattice is on the equator, which is along z . Therefore, the columns should lie well down on the $x-y$ plane, which is the substrate surface. It is well-known that mechanical shearing usually only offers unidirectional orientation to SCP samples, and thus, a ring pattern of 2D XRD will be obtained with the X-ray beam parallel to the shear direction. For P-8 (also for P-12, see the SI), the rotational disorder around the external force direction is largely suppressed, implying that the sample has good processability.

The a of the hexagonal lattice is somewhat close to double the estimated side-chain length. Therefore, while the flexibility due to the two methyleneoxy linkages promotes long-range ordering, the rigidity owned by the side-chain still largely controls the LC periodicity. The reconstructed relative electron density map of P-8 is presented in Figure 3d. The area with the lowest electron density (red colored) certainly belongs to alkyl tails, while the core of column with intermediate electron density (light-green circular area) should be filled with PS backbones. Unfortunately, the continuous electron density profile does not index the accurate size of PS core. Assuming that the PS backbone and the side chain possess a similar density of ~ 1 g/cm³, the diameter of the PS core (D_{PS}) can be roughly estimated to be ~ 2 nm, as indexed by the white circle in Figure 3d. The location of the circle is close to that of the electron density maximum. Away from the core area, the electron density decays monotonically along the radial direction, meaning that within a certain stratum the biphenyl groups are no longer packed in parallel but are sprayed. Overall, the column of Φ_h possesses a “core-shell-corona” structure, with the core of PS backbones, the shell of mesogens, and the corona of tails, respectively. The electron density map of P-12 (see the SI) is similar, whereas its longer tails enlarge the column diameter and form a more continuous phase of “corona”.

Considering that the hemiphasmidic side chain is slimmer than that of dendritic group, of particular interesting is how the packing behavior of P- n chains will be different from that of dendronized polymers. On the basis of the 2D XRD results and the molecular simulation, we take the value of ~ 0.44 nm as the average layer thickness of the side-chain, and thus the c -dimension of the hexagonal unit cell. Therefore, the number of repeating units (Z_{rep}) packed in a unit cell can be estimated as: $Z_{rep} = (N_A/M)(a^2 c \sin 60^\circ)\rho$, where N_A is the Avogadro's number, ρ is the density, and M is the molar mass of repeating unit. Taking the experimental densities (ρ_{exp} , see Table 1) of 1.02 and 0.95 g/cm³ for P-8 and P-12, the calculated values of Z_{rep} are 10.3 for P-8 and 8.4 for P-12, respectively, which are notably large.

For the Φ_h phases of dendronized polymers or mesogen-jacketed LC polymers, the building block is generally considered to be a single-chain cylinder, which is formed by warping the side chain around the chain backbone. It is also

suggested that the backbone can adopt a helical conformation.^{5b,6b} Taking this “single-chain model” for P-*n* (*n* ≥ 8), we should assume an individual segment containing ~10 repeating units to be compressed in an ~0.44 nm thick stratum. In this case, the atactic PS backbone will suffer a fully oblate conformation. Moreover, note that the PS core diameter is ~2 nm and the PS backbone and the biphenyl are tightly connected. Because the mesogens tend to align toward the outside, the PS backbone has to stay in the vicinity of the core/shell interface. This will result in a very low density in the core center, which is also not reasonable. Consequently, this “single-chain model” seems not to describe well the packing of P-*n* in the Φ_h phase.

Alternatively, as schematically drawn in Figure 4b, we propose a “multichain model” for the Φ_h phase. Namely, each

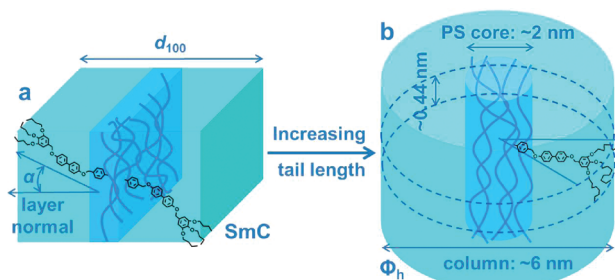


Figure 4. Schematic of the bilayer SmC (a) and the “multichain model” of column in Φ_h phase (b) of P-*n*. α is the tilt angle of the side chain in SmC. The blue curves represent the main-chain. Increasing tail length leads to the change of SmC to Φ_h . While the main-chain sublayer in smectic structure formed by many backbones, the core of the column in the Φ_h phase should also be able to contain more than one backbone.

column is constructed by a bundle of chains. This chain packing behavior can be understood along the line of microphase separation,² considering that the main chain of P-*n* is incompatible with the side chains. The smectic phase has somewhat a flat interface between main and side chains. Increasing the tail length leads to a larger volume fraction of the side chain, which is more wedge shaped. As a result, the flat interface becomes unfavorable eventually, resulting in the phase changing from smectic to Φ_h (Figure 4), which can be analogous to the lamella-to-cylinder transition of a block copolymer. While many chain backbones constitute the main-chain sublayer in smectic, it is also unnecessary for the column of SCP to contain only one chain in Φ phase. The possibility of more than one backbone laterally associated together in one column was mentioned before.⁶ Here, considering that the rodlike mesogens is tightly linked with the backbone, the large Z_{rep} value may be taken as an indication of several chains involved in the column. We further presume that the PS backbone is quite extended along the column axis because of the strong steric repulsive interactions between neighboring side-chains.¹⁴ Assuming that the projection of two repeating units on the chain axis is ~0.44 nm,^{7b-d} the bundle of P-8 and P-12 in the Φ_h phase contains ~5 and ~4 chains, respectively. Furthermore, there is a tendency to reduce Z_{rep} with increasing *n*. One may speculate that if the tail is large enough, the column of P-*n* might be built of a single-chain.

In summary, we synthesized a new hemiphasmidic SCP P-*n*. The side chain of P-*n* contains a central biphenyl linked to the PS backbone and the half-disk end group via methyleneoxy units. Upon increasing *n*, the phase of P-*n* changes from SmC

to Φ_h . The LC phases are long-range ordered, which may be attributed to the fact that the side chain can properly adjust its conformation and orientation during self-assembling. Benefiting from the chain structure, the LC domains of P-*n* can be easily oriented by shearing. The rotational disorder around the shear direction of the oriented Φ_h phase is rather low. Therefore, P-*n* exhibits quite good processability. The Φ_h phase most likely takes a bundle of chains rather than a single chain as its building block. This “multi-chain model” of Φ_h may represent a new type of self-assembly in SCP. However, this model requires more experimental and theoretical analysis. At this moment, the details of chain packing and dynamics are largely unknown. As the periodicity of LC structure can be tuned by side-chain size, one can expect that if a hemiphasmidic SCP bears a longer side chain, of which the chemical structure is precise, the periodicity of Φ_h can approach 10 nm. Further investigation on hemiphasmidic and also other SCPs with large side chains can pave a way, which is an alternative to block copolymer, toward precision fabrication of 2D ordered structures at ~10 nm length scale for advanced technology.

ASSOCIATED CONTENT

Supporting Information

Syntheses and characterizations of monomer and polymer; electron density reconstruction; and ^1H NMR, DSC, XRD data, and relative electron density maps. This material is available free of charge via the Internet at <http://pubs.acs.org>.

AUTHOR INFORMATION

Corresponding Author

*E-mail: eqchen@pku.edu.cn; shuangyang@pku.edu.cn.

Notes

The authors declare no competing financial interest.

ACKNOWLEDGMENTS

This work was supported by the National Natural Science Foundation of China (NNSFC Grants 20990232 and 21104001) and the MOST (2011CB606004).

REFERENCES

- (1) Whitesides, G. M.; Grzybowski, B. *Science* **2002**, 295, 2418–2421.
- (2) (a) Leibler, L. *Macromolecules* **1980**, 13, 1602. (b) Bates, F. S.; Fredrickson, G. H. *Annu. Rev. Phys. Chem.* **1990**, 41, 525–557. (c) Hamley, I. W. *The Physics of Block Copolymers*; Wiley: Chichester, U.K., 2009.
- (3) (a) Thurn-Albercht, T.; Schotter, J.; Kastle, C. A.; Emley, N.; Shibauchi, T.; Krusin-Elbaum, L.; Guarini, K.; Black, C. T.; Tuominen, M. T.; Russell, T. P. *Science* **2000**, 290, 2126–2129. (b) Cheng, J. Y.; Mayes, A. M.; Ross, C. A. *Nat. Mater.* **2004**, 3, 823–828. (c) Black, C. T. *ACS Nano* **2007**, 1, 147–150. (d) Park, S.; Lee, D. H.; Xu, J.; Kim, B.; Hong, S. W.; Jeong, U.; Xu, T.; Russell, T. P. *Science* **2009**, 323, 1030–1033.
- (4) (a) McArdle, C. B. *Side Chain Liquid Crystal Polymers*; Blackie: Glasgow, U.K., 1989. (b) Finkelmann, H.; Ringsdorf, H.; Wendorff, H. *Makromol. Chem.* **1978**, 179, 273–276. (c) Davidson, P. *Prog. Polym. Sci.* **1996**, 21, 893–950.
- (5) (a) Ungar, G. *Polymer* **1993**, 34, 2050–2059. (b) Rudick, J. G.; Percec, V. *Acc. Chem. Res.* **2008**, 41, 1641–1652. (c) Rosen, B. M.; Wilson, C. J.; Wilson, D. A.; Peterca, M.; Imam, M. R.; Percec, V. *Chem. Rev.* **2009**, 109, 6275–6540. (d) Chen, X. F.; Shen, Z. H.; Wan, X. H.; Fan, X. H.; Chen, E. Q.; Ma, Y. G.; Zhou, Q. F. *Chem. Soc. Rev.* **2010**, 39, 3072–3101. (e) Sheiko, S. S.; Sumerlin, B. S.; Matyjaszewski, K. *Prog. Polym. Sci.* **2008**, 33, 759–785.

- (6) (a) Percec, V.; Heck, J.; Tamazos, D.; Falkenberg, F.; Blackwell, H.; Ungar, G. *J. Chem. Soc., Perkin Trans. 1* **1993**, 2799–2811. (b) Kwon, Y. K.; Chvalun, S.; Schneider, A.-D.; Blackwell, J.; Percec, V.; Heck, J. A. *Macromolecules* **1994**, 27, 6129–6132.
- (7) (a) Zhou, Q. F.; Li, H. M.; Feng, X. D. *Macromolecules* **1987**, 20, 233–234. (b) Tu, H.; Wan, X.; Liu, Y.; Chen, X.; Zhang, D.; Zhou, Q.-F.; Shen, Z.; Ge, J. J.; Jin, S.; Cheng, S. Z. D. *Macromolecules* **2000**, 33, 6315–6320. (c) Yin, X. Y.; Ye, C.; Ma, X.; Chen, E. Q.; Qi, X. Y.; Duan, X. F.; Wan, X. H.; Cheng, S. Z. D.; Zhou, Q. F. *J. Am. Chem. Soc.* **2003**, 125, 6854–6855. (d) Ye, C.; Zhang, H. L.; Huang, Y.; Chen, E. Q.; Lu, Y. L.; Shen, D. Y.; Wan, X. H.; Shen, Z. H.; Cheng, S. Z. D.; Zhou, Q. F. *Macromolecules* **2004**, 37, 7188–7196.
- (8) (a) Schlüter, A. D.; Rabe, J. P. *Angew. Chem., Int. Ed.* **2000**, 39, 20. (b) Frauenrath, H. *Prog. Polym. Sci.* **2005**, 30, 325–384. (c) Das, J. J.; Yoshida, M.; Fresco, Z. A.; Choi, T.-L.; Fréchet, J. M. J.; Chakraborty, A. K. *J. Phys. Chem. B* **2005**, 109, 6535–6543. (d) Zhang, B. Z.; Wepf, R.; Fischer, K.; Schmidt, M.; Besses, S.; Lindner, P.; King, B. T.; Sigel, R.; Schurtenberger, P.; Talmon, Y.; Ding, Y.; Kroger, M.; Halperin, A.; Schlüter, A. D. *Angew. Chem., Int. Ed.* **2011**, 50 (3), 737–740.
- (9) Lin, C.; Ringsdorf, H.; Ebert, M.; Kleppinger, R.; Wendorff, J. H. *Liq. Cryst.* **1989**, 5, 1841–1847.
- (10) (a) Percec, V.; Heck, J. *Polym. Bull.* **1990**, 24, 255–262. (b) Percec, V.; Heck, J.; Ungar, G. *Macromolecules* **1991**, 24, 4957–4962.
- (11) (a) Nguyen, H.-T.; Destrade, C.; Malthête, J. *Adv. Mater.* **1997**, 9, 375–388. (b) Gharbia, M.; Gharbi, A.; Nguyen, H.-T.; Malthête, J. *Curr. Opin. Colloid Interface Sci.* **2002**, 7, 312–325.
- (12) (a) Percec, V.; Yourd, R. *Macromolecules* **1988**, 21, 3379–3386. (b) Percec, V.; Yourd, R. *Macromolecules* **1989**, 22, 524–537.
- (13) (a) Lee, M.; Cho, B. K.; Zin, W. C. *Chem. Rev.* **2001**, 101, 3869–3892. (b) Olsen, B. D.; Segalman, R. A. *Mater. Sci. Eng. R* **2008**, 62, 37–66. (c) Lotz, B.; Cheng, S. Z. D. *Polymer* **2005**, 46, 577–610.
- (14) Fredrickson, G. H. *Macromolecules* **1993**, 26, 2825–2831.